RSC Advances

ROYAL SOCIETY OF CHEMISTRY

www.rsc.org/advances

RSC Adv.

RSCPublishing

paper

Hybrid of CoOOH nanorods with carbon nanotubes as superior positive electrode material for supercapacitors

Cite this: DOI: 10.1039/x0xx00000x

Lei Zhu,[a,b,c] Wenyi Wu,[b] Xiaowei Wang,[b] Xiongwei Wu*[a], Weiping Tang*[c] and Yuping Wu*[a,b]

Received 00th January 2014,
Accepted 00th January 2014

DOI: 10.1039/x0xx00000x

www.rsc.org/

Abstract: The hybrid of CoOOH nanorods with conductive MWCNTs is successfully prepared. Due to the introduction of MWCNTs, the diameter of the CoOOH nanorods is smaller than that of pristine CoOOH nanorods. Because of the conductive nanostructure network and smaller diameter of the CoOOH nanorods, it exhibits high capacitance, good high-rate capability and excellent cycling performance as a positive electrode for supercapacitors in a 0.5 mol L^{-1} KOH aqueous electrolyte. Its specific capacity is 312 F g^{-1} at the current density of 1 A g^{-1}, and 182 F g^{-1} even at the current density of 10 A g^{-1}. After 10 000 full cycles, the capacitance retention is 97%. The hybrid is of great promise for practical application.

1. Introduction

Various types of energy storage devices like lithium ion batteries,[1] aqueous rechargeable lithium batteries and supercapacitors[2,3] have been developed to satisfy the ever-increasing need for sustainable energies. Among them, supercapacitors have become a promising energy storage device due to its virtue of high power densities and long cycling life.[4-6] However, its major disadvantage is the low energy density. RuO_2 attracted great interest initially due to its high specific capacitance,[7] but the possibility to be commercialized in most applications is remote because of its high cost and environmental unfriendliness. In attempt to develop economical electrodes, series of metal oxides such as MnO_2, Co_3O_4, NiO_x, SnO_2, MoO_3, V_2O_5 and intercalation compounds such as M_xMnO_2 (M=Li, Na or K) [8-11] have been investigated. The energy densities of aqueous supercapacitors have been markedly improved. However, further increase is still needed.

Recently, CoOOH was also studied for the same reason.[12-14] However, the low conductivity makes its practical capacitance very low (< 200 F g^{-1}). So the key strategy to improving its electrochemical properties is to increase its electronic conductivity. In recent decades, carbon materials are not only one of the best choices in the aspect of facile fabrication and high electronic conductivity but also a promising electrode material because of their high stability.[15] As a result, carbon materials like activated carbon black,[16] mesoporous carbon[17] and carbon nanotubes[18] are used to form nanocomposites with transitional metal compounds. It is expected that this combination can take the advantages both of the high pseudocapacitance of transition metal compounds and the stable double-layer capacitance of carbon materials, and much enhanced supercapacitive performance is achieved. For this purpose, some highly conductive carbon materials have been brought into cobalt compounds to enhance their performance.[19] In addition, preparing nanostructured materials and depositing them on some conductive substrates like indium tin oxide (ITO)-coated glass, [20] nickel foam, [21] and graphene membrane[22] have been studied to increase its conductivity, resulting in the capacitance promotion. However, the active materials could easily be detached from the substrate due to their volume change during the charging/discharging process, and their cycling performance is not good. So, a superior solution is, combine some conductive materials with CoOOH closely, constructing a synergistic effect.

Here we designed and prepared a hybrid of CoOOH nanorods with multi-walled carbon nantubes (MWCNTs). The MWCNTs in the hybrid can increase the electronic conductivity to enhance the redox reactions of CoOOH, leading to an markedly increased capacitance, 312 F g^{-1} at the current density of 1 A g^{-1} in 0.5 mol L^{-1} KOH aqueous electrolyte, and the CoOOH nanorods provide a good buffer for volume change, leading to an excellent cycling performance, 97% capacitance retention after 10 000 full cycles.

2. Experimental

Synthesis of the hybrid of CoOOH nanorods with MWCNTs

Multiwall carbon nanotubes (MWCNTs) were dispersed in 6 M HNO_3 for 2 h with sonication to remove the impurities. Next, a certain amount of acid-treated MWCNTs were dispersed into an

[a] College of Science, Hunan Agriculture University, Changsha, Hunan 410128, PR China Email: wxwcsu05@aliyun.com

[b] *New Energy and Materials Laboratory (NEML), Department of Chemistry & Shanghai Key Laboratory of Molecular Catalysis and Innovative Materials, Fudan University, Shanghai 200433, PR China. E-mail: wuyp@fudan.edu.cn; Fax: +86-21-5566 4223; Tel: +86-21-5566 4223*

[c] *Shanghai Institute of Space Power-Sources (SISP), Shanghai Academy of Spaceflight Technology, Shanghai 200233, PR China. Email: wptang1962@gmail.com; Tel: +86-21-24187672*

aqueous solution of $Co(NO_3)_2 \cdot 6H_2O$ (0.04 mol L^{-1}) and $CO(NH_2)_2$ (0.2 mol L^{-1}), after sonication and agitation for 2 h separately, the mixture was transferred to a Teflon-lined autoclave and maintained at 95 °C for 8 h.[22] After cooling to room temperature, the suspension (the hybrid of MWCNTs and cobalt-hydroxide-carbonate) was oxidized by H_2O_2 at 90 °C for 4 h to turn Co(II) to Co(III), and then the targeted hybrid of CoOOH nanorods with MWCNTs was achieved. In addition, the pristine CoOOH nanorods were also prepared by the same method without adding the MWCNTs.

Materials characterization

Crystal structures of the sample X-ray diffraction (XRD) patterns were measured by a Rigaku D/MAX-IIA X-ray diffractometer with Cu-K_α radiation. Scanning electron micrographs (SEM) and transmission electron micrographs (TEM) were used to characterize the morphology of the hybrid of CoOOH nanorods with MWCNTs. The micrographs were obtained on a Philips XL30 scanning electron microscope and a JEOL JEM-2010 transmission electron microscope, respectively. Fourier Transform infrared spectroscopy (FTIR) was used to analyze the changes of MWCNTs before and after H_2O_2 treatment in the frequency range of 3750-900 cm^{-1}. The MWCNTs samples were mechanically mixed with the dried KBr powder and pressed into discs shape for test.

Electrochemical test

The electrochemical tests were carried out in a three-electrode system with 0.5 mol L^{-1} KOH solution as the electrolyte. The hybrid of CoOOH nanorods with MWCNTs mixed with acetylene black and poly(tetrafluoroethylene) (PTFE) in a weight ratio of 8:1:1 was used as the working electrode. The substrate used for working electrode is nickel foil, and in all tests, the quality of the active material loading on the substrate was precisely weighted, about 1.8 mg, the area of cathode electrode is 2 cm^2, corresponding to 0.9 mg/cm^2. In the meanwhile, a nickel foil was used as the counter electrode and a saturated calomel electrode (SCE) as the reference electrode. Cyclic voltammetry (CV) was investigated by a CHI 660D electrochemical station. LAND battery test system was employed to test galvanostatic charge-discharge and the cycling performance. A potential window in the range from 0 to 0.5 V was used in all the measurements. The electrochemical impedance spectroscopy (EIS) was conducted at the frequency of 0. 1 Hz.

3. Results and discussion

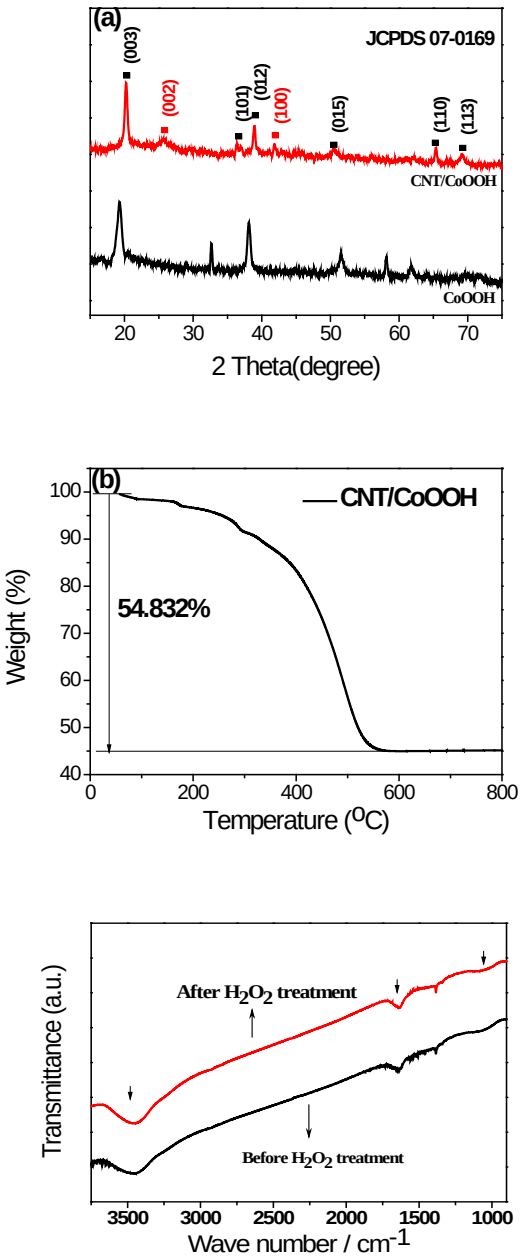

Fig. 1 (a) XRD patterns of the pristine CoOOH and the hybrid of CoOOH nanorods with MWCNTs, (b) TGA curve of the hybrid and (c) FTIR of the pristine MWCNTs before and after H_2O_2 treatment.

X-ray diffraction patterns of the pristine CoOOH and the hybrid of CoOOH nanorods with MWCNTs (Fig. 1a) present that the pristine CoOOH and the CoOOH in the hybrid exist in hexagonal rhomb-centered phase (JCPDS 07-0169) without any impurities.[23] In the case of the hybrid, the peaks at 26.2° and 43.2° correspond to the (002) and (100) planes of MWCNTs, respectively, which can be assigned to the hexagonal carbon (JCPDS No. 26-1079).[24] No other miscellaneous peaks were detected in this pattern, confirming that the composite materials are well crystallized. Thermogravimetric analysis (TGA) (Fig. 1b) suggests that the amount of CoOOH

present in the hybrid is about 50 wt.% by assuming that the remaining product after the TGA measurement is pure Co_3O_4.[25] Fig. 1c shows the FTIR of the pristine MWCNTs before and after H_2O_2 treatment at 90 °C for 4 h. There is not much evident difference change in the functional groups on the MWCNTs including hydroxyl (–OH, 3450 cm^{-1}), carbonyl (–C=O, 1630 cm^{-1}; C–O, 1170 cm^{-1}) and unsaturated bonds of graphitic structures (1630 cm^{-1}), whose absorption peaks are marked by arrows. This suggests that the oxidation is mainly valid for Co(II), which is turned into Co(III). These functional groups on the MWCNTs from the acid treatment might can serve as efficient electron pathways.[26,27]

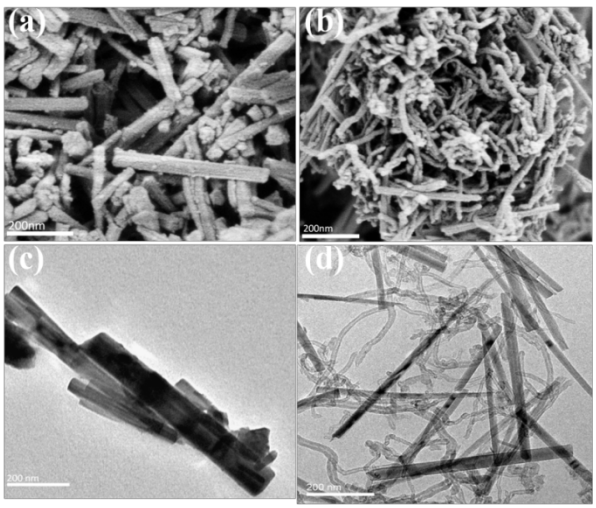

Fig. 2 Characterization of the pristine CoOOH nanorods and the hybrid. SEM micrographs of (a) the pristine CoOOH and (b) the hybrid, and TEM micrographs of (c) the pristine CoOOH and (d) and the hybrid.

Scanning electron micrographs (SEM) of the pristine CoOOH nanorods and the hybrid are shown in Fig. 2a and 2b, respectively. The pristine CoOOH exists in rod-like nanostructure with a diameter of 20 nm and a length of about 500 nm. The hybrid presents an interwoven network structure of CoOOH nanorods with MWCNTs. The TEM micrograph of the pristine CoOOH nanorods (Fig. 2c) is in agreement with the above SEM micrographs, and that of the hybrid (Fig. 2d) further confirm that the CoOOH nanorods and the MWCNTs are intertwined with each other completely, forming a network structure with good electronic conductive paths due to the outstanding conductivity of the MWCNTs network. Furthermore, from the comparison of Fig. 2c with Fig. 2d, it is interesting to note that the diameter of the CoOOH nanorods is decreased from 20 nm to approximately 10 nm after the adding of the MWCNTs. Perhaps the conductive nanostructure network could significantly prevent the reunion of nanoparticles during the nucleation progress, leading to the thinner CoOOH nanorods. The schematic illustration of the growth process is shown in Fig. 3.

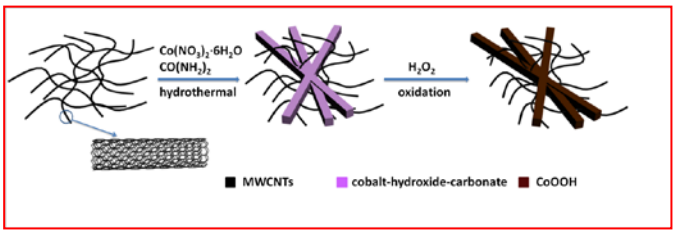

Fig. 3 Schematic illustration of the preparation process of the hybrid of CoOOH nanorods with MWCNTs.

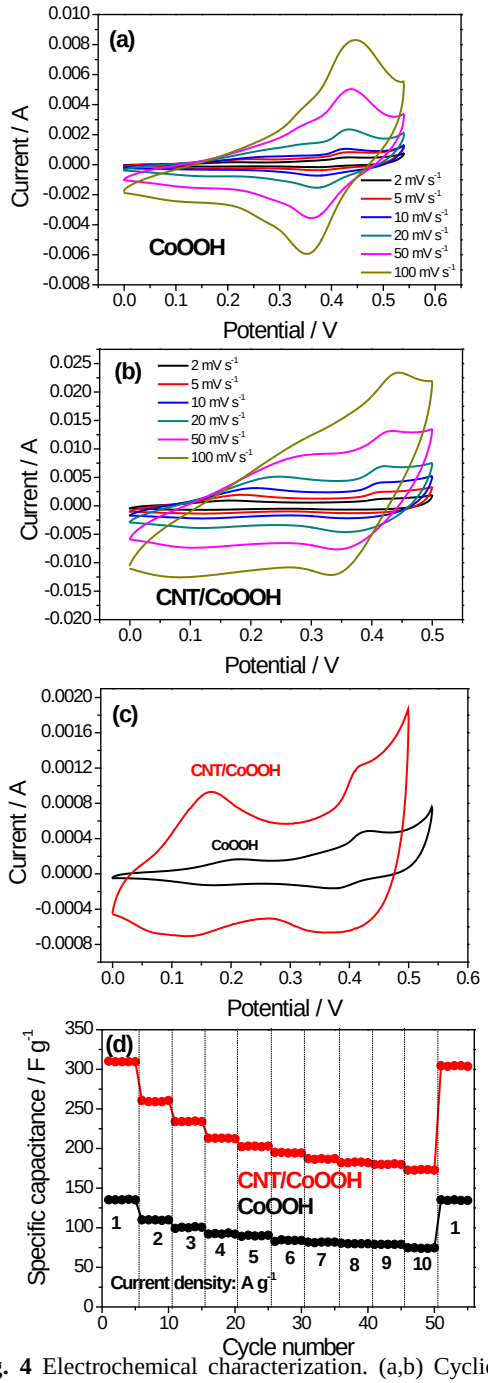

Fig. 4 Electrochemical characterization. (a,b) Cyclic voltammetric (CV) curves of the pristine CoOOH and the hybrid of CoOOH nanorods with MWCNTs at different scan rates, (c) comparison of

the CV curves between the pristine CoOOH and the hybrid at the scan rate of 2 mV s^{-1}, and (d) comparison of capacitances between the pristine CoOOH and the hybrid at different current densities.

The electrochemical properties of the as-prepared samples evaluated by a three electrode system in 0.5 mol L^{-1} KOH aqueous solution with a nickel foil as the counter electrode and a saturated calomel electrode (SCE) as the reference electrode are shown in Fig. 4. The CV curves of the pristine CoOOH nanorods and the hybrid at different scan rates (2-100 mV s^{-1}) (Fig. 4a and 4b) present symmetric shapes proving the high reversibility of the Faradaic reactions, which will contribute to pseudo-capacitance. The two distinct pairs of redox peaks correspond to the reactions between Co(II)/Co (III) and Co(III)/Co(Ⅳ), respectively. On the basis of the reported electrochemical reactions of $Co(OH)_2$ and Co_3O_4, the possible redox reactions can be described as follows: [28,29]

$$CoOOH + H_2O + e^- \leftrightarrow Co(OH)_2 + OH^- \quad \text{(lower potential)} \quad (1)$$

$$CoO_2 + H_2O + e^- \leftrightarrow CoOOH + OH^- \quad \text{(higher potential)} \quad (2)$$

With the increase of the scan rate, the current densities of the two CV curves increase, indicating their good capacitive behaviors. Compared with the pristine CoOOH, the hybrid shows a much larger current density at the same scan rates. At the scan rate of 2 mV s^{-1}, one of the two pairs of the redox peaks for the hybrid at lower potential becomes more distinct. Markedly, the area of the CV curves of the hybrid is drastically expanded, indicating a much larger capacitance. That is to say, this hybrid enhanced the Faradaic reactions of CoOOH, indicating faster electron and ion transport, which is benefit from the incorporated MWCNTs into the CoOOH nanorods, promoting the conductivity of the electrode and accelerating the ion diffusion. This is also consistent with the results in Fig. 4d. The hybrid presents a specific capacitance of 312 F g^{-1} at the current density of 1 A g^{-1}, much higher than that of the pristine CoOOH (136 F g^{-1}) at the same current density. The specific capacitance is calculated according to the following equation:[30]

$$C = I \Delta t / (m \Delta V) \quad (3)$$

where I (mA) is discharge current, Δt (s) is discharge time, ΔV (V) is the potential window and m (mg) is mass of the active material. The weight refers to that of CoOOH, which is 50 wt.% of that of the hybrid, according to the TGA test. In addition, whether at low or high current densities from 1 A g^{-1} to 10 A g^{-1}, the hybrid shows higher capacitance than the pristine CoOOH. As mentioned above, the MWCNTs network provides higher electronic conductivity, favoring the redox reactions as shown in Eqs. (1) and (2) that contribute to the large pseudo-capacitance. Another reason is perhaps due to the smaller diameters of the CoOOH nanorods in the hybrid, which provide more surface sites for the redox reactions and shorten the distance for ion diffusion. As reported, at lower current density, ions can easily penetrate into almost every available site of the electrode material due to sufficient time; while at higher current density, only the outer part of the electrode material can contact quickly with ions.[31, 32] That is to say, owing to the limited accessible areas for ions diffusion, with the increase of current density, the specific capacitance will decrease gradually. However, in the case of the hybrid, its specific capacitance still maintains 182 F g^{-1} even at the high current density of 10 A g^{-1}. When the current density is back to 1 A g^{-1}, the capacitance is almost recovered, indicating good reversibility of CoOOH nanorods.

The galvanostatic charge/discharge curves and cycling behavior of the pristine CoOOH nanorods and the hybrid in 0.5 mol l^{-1} KOH between 0 and 0.5 V (vs. SCE) are shown in Fig. 5. Compared with the pristine CoOOH electrode, the charge/discharge curves of the hybrid is much more symmetric, indicating lower internal resistance due to the introduction of the MWCNTs network. At the same low current density of 1 A g^{-1} (Fig. 5c), the hybrid can be discharged for longer time, which is consistent with the former CV results, larger capacitance for the hybrid. From the discharge curves of the hybrid at the current density of 1 A g^{-1}, two stages ranging from 0.1-0.2 V and 0.4-0.5 V, corresponding to the reactions (1) and (2), respectively, can be clearly discerned, which are also in accordance with the above CV curves.

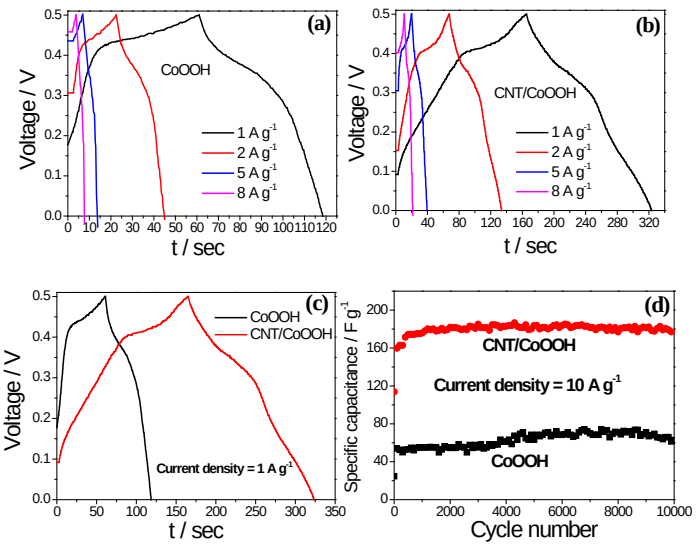

Fig. 5 Galvanostatic charge and discharge characterization. (a,b) Constant current charge/discharge curves of the pristine CoOOH and the hybrid of CoOOH nanorods with MWCNTs at different current densities, (c) comparison between the charge/discharge curves of the pristine CoOOH and the hybrid at the current density of 1 A g^{-1}, and (d) cycling performance of the pristine CoOOH and the hybrid at the current density of 10 A g^{-1}.

Fig. 5d reveals the cycling performance of the pristine CoOOH nanorods and the hybrid of CoOOH nanorods with MWCNTs at the current density of 10 A g^{-1}. Firstly, during the initial 200 cycles, the capacitance for both the pristine CoOOH nanorods and the hybrid increase gradually, this is evidently due to the initial activation process for the immersion of the electrolyte into the inner of the active materials.[33, 34] On the other hand, after combined with the MWCNTs, there is a significant growth of specific capacitance. After stabilizing, the composite electrode can deliver a reversible capacity of 182 F g^{-1} at the current density of 10 A g^{-1}, about 100 F g^{-1} higher than that of the pristine CoOOH electrode. Moreover, it can

be seen that the hybrid exhibits much better cycling performance than that of the pristine CoOOH electrode. The capacitance of the hybrid remains 177 F g^{-1} for the 10 000th cycle, which corresponds to 97% capacity retention. However, the capacitance of the pristine CoOOH electrode fades more quickly from 74 F g^{-1} to 62 F g^{-1} after 10 000 cycles (84% capacity retention), illustrating the configuration decorated by MWCNTs is more stable, causing the excellent long-term cycling performance.

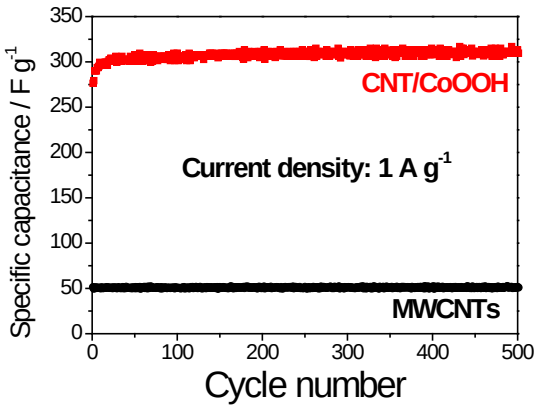

Fig. 6 The comparison of the specific capacitance between the pristine MWCNTs and the hybrid of CoOOH nanorods with MWCNTs at the current density of 1 A g^{-1}.

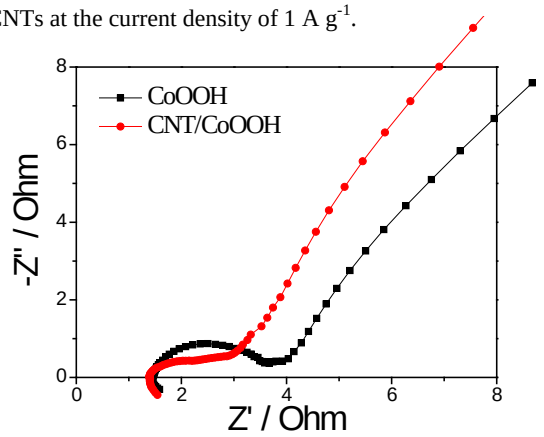

Fig. 7 Electrochemical impedance spectra (EIS) of the pristine CoOOH and the hybrid of CoOOH nanorods with MWCNTs at the frequency of 0.1 Hz.

The comparison of the specific capacitance between the pristine MWCNTs and the hybrid under the same conditions (0.5 mol l^{-1} KOH between 0 and 0.5 V) at a current density of 1 A g^{-1} is shown in Fig. 6. The pristine MWCNTs deliver a specific capacitance of only 50 F g^{-1} at a current density of 1 A g^{-1}, which contributes very little to the electrochemical property of the hybrid of CoOOH nanorods with MWCNTs (312 F g^{-1}). This means the high capacitance of the hybrid is significantly derived from the CoOOH nanorods while the MWCNTs may act as an adjuvant to construct a conductive network.

The EIS curves (Fig. 7) were recorded in the frequency of 0.1 Hz for further understanding of the electrochemical behavior of the pristine CoOOH and the hybrid of CoOOH nanorods with MWCNTs. The impedance spectrum is composed of a semicircle in the high frequency region and a nearly linear part in the low frequency region. The diameter of the semicircle is probably related to the charge transfer resistance. It is seen that the internal resistance of the hybrid is about 1.2 Ω, smaller than that of the pristine CoOOH (2 Ω), showing good electronic contact between the active material and the electrolyte. In addition, the charge transfer resistance of the hybrid is also smaller than that of the pristine CoOOH. These results show that the introduction of CNTs enables a much easier charge transfer at the electrode/electrolyte interface, and consequently decreases the overall supercapacitor internal resistance, resulting in a significant improvement in the electrochemical performance.

The above superior electrochemical performance of the hybrid can be ascribed to the following reasons: (1) MWCNTs-wiring can modify the connection of CoOOH nanorods to conductive network which can reduce particle reunion chance and further decrease the size of active particles, fully improving high power characteristics of the electrode materials and shortening the ion diffusion distance for redox reactions; (2) Due to high electronic conductivity character of the MWCNTs, the hybrid can provide greatly rapid electron transference, resulting in the significant improvement in the kinetic performance of electrochemical reversible reactions. This also ensure high rate performance; and (3) the superior stable mechanical stability of the MWCNTs causes the prepared hybrid of CoOOH nanorods with MWCNTs electrode to be more stable and flexible during cycling, and to buffer the volume change of the active materials during the charge/discharge process. Consequently, the hybrid exhibits high reversible capacitance, good high-rate capability and excellent cycling performance.

4. Conclusions

In summary, a hybrid of CoOOH nanorods with MWCNTs is successfully prepared. It delivers a high specific capacitance of 312 F g^{-1} at the current density of 1 A g^{-1}, much higher than that of the pristine CoOOH (136 F g^{-1}) at the same current density. In addition, the hybrid presents very good rate performance. Even at the current density of 10 A g^{-1}, 182 F g^{-1} of the capacitance could be obtained. Besides, the retention of capacitance is about 97% after 10000 full cycles at a high current density of 10 A g^{-1}, revealing an excellent cycling stability. The hybrid of CoOOH nanorods with MWCNTs electrode is of great promise for commercial application in aqueous supercapacitors.

Acknowledgements

Financial support from China National Funds for Distinguished Young Scholars (NSFC) is greatly appreciated.

Notes and References

1 (a) J. Tollefson, *Nature*, 2008, **456**, 436-440; (b) L.J. Fu, K. Tang, C.C. Chen, L. Liu, X. Guo, Y. Yu, J. Maier, *Nanoscale*, 2013, **5**, 11568; (c) Y.S. Zhu, S.Y. Xiao, Y. Shi, Y.Q. Yang, Y.Y. Hou, Y.P. Wu, *Adv. Energy Mater.*, 2014, **4**, 1300647.

2 (a) W. Tang, Y. Y. Hou, F. X. Wang, L. L. Liu, Y. P. Wu and K. Zhu, *Nano Lett.*, 2013, **13**, 2036-2040; (b) W. Tang, Y.S. Zhu,

Y.Y. Hou, L.L. Liu, Y.P. Wu, K.P. Loh, H.P. Zhang and Kai Zhu, *Energy Environ. Sci*., 2013, **6**, 2093-2104; (c) Z. Chang, Y.Q. Yang, M.X. Li, X.W. Wang, Y.P. Wu, *J. Mater. Chem. A*, 2014, **2**, 10739-10855; (d) J.C. Arrebola, Á. Caballero, L. Hernán, and J. Morales, *Energy Fuels* 2013, **27**, 7854-7857.

3 (a) P. Simon and Y. Gogotsi, *Nat. Mater.*, 2008, **7**, 845-854; (b) B. G. Choi, S. J. Chang, H. W. Kang, C. P. Park, H. J. Kim, W. H. Hong, S. G. Lee and Y. S. Huh, *Nanoscale*, 2012, **4**, 4983-4988; (c) F. X. Wang, S. Y. Xiao, Y. Y. Hou, C. L. Hu, L. L. Liu and Y. P. Wu, *RSC Adv.*, 2013, **3**, 13059-13084.

4 J. X. Feng, Q. Li, X. F. Lu, Y. X. Tong and G. R. Li, *J. Mater. Chem. A*, 2014, **2**, 2985-2992.

5 J. R. Miller and P. Simon, *Science*, 2008, **321**, 651-652.

6 R. Väli, A. Laheäär, A. Jänes and E. Lust, *Electrochim. Acta.*, 2014, **121**, 294-300.

7 (a) D.P. Dubal, G.S. Gund, R. Holze, H.S. Jadhav, C.D. Lokhande, C.J. Park, *Electrochim. Acta*, 2013, **103**, 103-109; (b) R. Vellacheri, V. K. Pillai and S. Kurungot, *Nanoscale*, 2012, **4**, 890-896.

8 (a) Q. T. Qu, P. Zhang, B. Wang, Y. H. Chen, S. Tian, Y. P. Wu and R. Holze, *J. Phys. Chem. C*, 2009, **113**, 14020-14027; (b) L. Hou, C. Yuan, L. Yang, L. Shen, F. Zhang and X. Zhang, *RSC Adv.*, 2011, **1**, 1521-1526.

9 (a) I. Shakir, Z. Ali, J. Bae, J. J. Park and D. J. Kang, *Nanoscale*, 2014, **6**, 4125-4130; (b) H. T. Cui, Y. Liu, W. Z. Ren, M. M. Wang and Y. N. Zhao, *Nanotechnology*, 2013, **24**, 345602-345607.

10 (a) W. Tang, L. L. Liu, S. Tian, L. Li, Y. B. Yue, Y. P. Wu and K. Zhu, *Chem. Commun.*, 2011, **47**, 10058 - 10060; (b) Y. Liu, B. H. Zhang, Y. Q. Yang, Z. Chang, Z. B. Wen and Y. P. Wu, *J. Mater. Chem. A*. 2013, **1**, 13582-13587; (c) Q. T. Qu, Y. S. Zhu, X. W. Gao and Y. P. Wu, *Adv. Energy Mater.*, 2012, **2**, 950- 955.

11 Q. T. Qu, Y. Shi, S. Tian, Y. H. Chen, Y. P. Wu and R. Holze, *J. Power Sources*., 2009, **194**, 1222-1225; (b) B. H. Zhang, Y. Liu, Z. Chang, Y. Q. Yang, Z. B. Wen, Y. P. Wu and R. Holze, *J. Power Sources*, 2014, **253**, 98 - 103.

12 X. Wang, A. Sumboja, M. Lin, J. Yan and P. S. Lee, *Nanoscale*, 2012, **4**, 7266-7272.

13 Z. P. Liu, R. Z. Ma, M. Osada, K. Takada and T. Sasaki, *J. Am. Chem. Soc.*, 2005, **127**, 13869-13874.

14 L. Cao, F. Xu, Y. Y. Liang and H. L. Li, *Adv. Mater.*, 2004, **16**, 1853-1857.

15 M. Gong, Y. G. Li, H. L. Wang, Y. Y. Liang, J. Z. Wu, J. G. Zhou, J. Wang, T. Regier, F. Wei and H. J. Dai, *J. Am. Chem. Soc.*, 2013, **135**, 8452-8455.

16 X. J. He, Y. J. Geng, S. Oke, K. Higashi, M. Yamamoto and H. Takikawa, *Synthetic Metals*, 2009, **159**, 7-12.

17 X. J. He, K. Xie, R. C Li and M. B. Wu, *Materials Letters*, 2014, **115**, 96-99.

18 R. R. Bi, X. L. Wu, F. F. Cao, L. Y. Jiang, Y. G. Guo and L. J. Wan, *J. Phys. Chem. C*, 2010,**114**, 2448-2451.

19 K. Naoi, S. Ishimoto, J. Miyamoto and W. Naoi, *Energy Environ. Sci.*, 2012, **5**, 9363-9373.

20 (a) C. Y. Yan, H. Jiang, T. Zhao and C. Z. Li, *J. Mater. Chem.*, 2011, **21**, 10482-10488; (b) H. J. Zheng, F.Q. Tang, M. Lim, T. Rufford, A. Mukherji, L. Z. Wang and G. Q. Lu, *J. Power Sources*, 2009, **193**, 930-934.

21 E. Hosono, S. Fujihara, I. Honma, M. Ichihara and H. Zhou, *J. Power Sources*, 2006, **158**, 779-783.

22 L. Li, G. M. Zhou, X. Y. Shan, S. F. Pei and F. Li, *J. Power Sources*, 2014, **255**, 52-58.

23 B. Y. Geng, F. M. Zhan, H. Jiang, Z. J. Xing and C. H. Fang, *Crystal Growth & Design*, 2008, **8**, 3497-3500.

24 M. Xu, D. N. Futaba, M. Yumura and K. J. Hata, *Nano Lett.*, 2011, **11**, 3279-3284.

25 S. K. Meher and G. R. Rao, *J. Phys. Chem. C*, 2011, **115**, 15646-15654.

26 M. Longhi and L. Formaro, *Electrochem. Commun.*, 2002, **4**, 123-127.

27 F. Barde, M. R. Palacin, B. Beaudoin, A. Delahaye-Vidal and J. M. Tarascon, *Chem. Mater.*, 2004, **16**, 299-306.

28 T. Yan, Z. J. Li, R. Y. Li, Q. Ning, H. Kong, Y. L. Niu and J. K. Liu, *J. Mater. Chem. A*, 2012, **22**, 23587-23592.

29 L. L. Jiang, Z.J. Fan, *Nanoscale*, 2014, 6, 1922-1945.

30 F. C. Meng, J. N. Zhao, Y. T. Ye, X. H. Zhang and Q.W. Li, *Nanoscale*, 2012, **4**, 7464-7468.

31 R. Jackson, B. Domercq, R. Jainet, B. Kippelen, S. Graham, *Adv. Funct. Mater.*, 2008,**18**, 2548-2554.

32 Y. Hou, L. Y. Chen, P. Liu, J. L. Kang, T. Fujita and M. W. Chen, *J. Mater. Chem. A*, 2014, **2**, 10910-10916.

33 R. B. Rakhi, W. Chen, D. Cha and H. N. Alshareef, *Nano Lett.*, 2012, **12**, 2559-2567.

34 C. Z. Yuan, J. Y. Li, L. R. Hou, X. G. Zhang, L. F. Shen and X. W. Lou, *Adv. Funct. Mater.*, 2012, **22**, 4592-4597.

Table of content:

Hybrid of CoOOH nanorods with carbon nanotubes as superior positive electrode material for supercapacitors

Lei Zhu, Wenyi Wu, Xiaowei Wang, Xiongwei Wu, Weiping Tang and Yuping Wu*

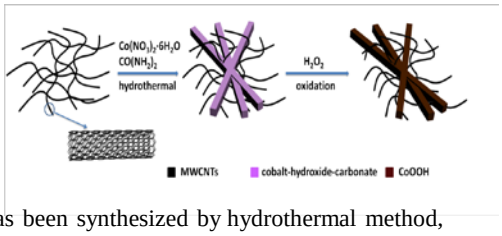

A hybrid of CoOOH nanorods with MWCNTs has been synthesized by hydrothermal method, exhibiting high reversible capacitance, good high-rate capability and excellent cycling performance.